Novel experimental system as an alternative to animal experiments to study the skin permeation of drugs

Toshinobu Seki, Tatsuya Sashida, Shinji Oshima, Yuya Egawa, Hiroko Nakagawa, Osamu Hosoya and Kazuhiko Juni

Faculty of Pharmaceutical Sciences, Josai University

Corresponding author:
Toshinobu Seki
Faculty of Pharmaceutical Sciences, Josai University,
1-1 Keyakidai, Sakado, Saitama 350-0295, Japan
Tel 049-271-7686
Fax 049-271-7714
sekt1042@josai.ac.jp

Abstract

A skin-mimicking artificial membrane consisting of a silicone membrane as a model stratum corneum and laminated dialysis membranes as a model of viable skin was prepared to imitate the layered structure of skin. The permeability of flurbiprofen (FP) through the laminated membranes agreed with that calculated, suggesting that the interfacial resistance between each membrane was negligible. When the FP concentration in the laminated membranes was determined by microdialysis, the observed concentration was similar to that calculated according to Fick's law of diffusion. When bovine serum albumin (BSA) solution was placed between the dialysis membranes to mimic the protein leaching in skin, the FP permeation profiles through the membranes showed a long lag-time without dependence on the depth of the region of the inserted BSA from the surface. However, the FP concentration-time profiles in a region between the membranes showed dependence on the region of the inserted BSA. Since the FP concentration in the region and the permeation rates at steady-state were similar to those without BSA solution, BSA could act as a capacity factor to the delayed reaching to a steady-state. The skin mimicking laminated membranes will be useful to evaluate drug permeation quantitatively and to imitate some events which can happen in inflamed tissues in skin without requiring animals.

Key words: skin absorption, microdialysis, artificial membrane, zero net flux, protein binding

Introduction

Topical formulations can be categorized into two types according to their target site of action. One involves the systemic action of drugs which are absorbed from the cutaneous microvessels while the other exhibits local effects in the skin and subcutaneous tissues (Russell and Guy, 2009). Since the drug disposition in the skin is important for both types of formulations, evaluation of the drug concentration profiles in skin is very helpful for formulation design (Touitou *et al.*, 1998). *In vitro* skin permeation experiments using excised skin are the most popular experimental methods to study skin absorption of drugs. Since only a few pieces of excised skin can be obtained from one animal, the *in vitro* experimental systems are useful to reduce the use of experimental animals. However, the *in vitro* experimental systems are not suitable for evaluating the drug concentration profiles in skin because of the lack of local blood flow and physiological response (Roberts and Cross, 1999). Changes in blood flow and inflammation in the local tissue can affect the drug concentration in skin (Ortiz *et al.*, 2008; Clough *et al.*, 2002). Although such changes occur in *in vivo* systems, the *in vivo* experimental systems have a number of problems, such as the detection limit, reproducibility and number of animal used (Morimoto *et al.*, 2000; Shukla *et al.*, 2009; Ortiz *et al.*, 2009). Alternatives to animal testing and experimentation are valuable not only to reduce the use of experimental animals but also to allow the control of experimental conditions. Therefore, a new skin-mimicking *in vitro* experimental system as an alternative experimental technique, which can artificially create local inflammation, will be useful for basic studies of the skin absorption of drugs.

Skin consists of an epidermis and dermis, and the outer layer of the epidermis is the stratum corneum. The stratum corneum is composed of dead keratinocyte layers and acts as a permeation barrier to foreign material. Since the corneocytes are surrounded by intercellular lipids, the

stratum corneum is a lipophilic membrane. Different types of artificial membrane have been evaluated as a model of the stratum corneum to predict the steady-state permeation rate of drugs through skin (de Jager *et al.*, 2005; Ottaviani *et al.*, 2006). On the other hand, the viable epidermis and dermis have a high water content like a hydro gel and these may not work as diffusion barriers in most cases. However, since the physiological changes occur in the viable skin, the condition of the layers can directly affect the concentration profiles of drugs in skin (Roberts and Cross, 1999; Ortiz *et al.*, 2008). Therefore, the new skin-mimicking membrane system should be a laminated structure and should be able to reproduce physiological changes in skin.

In this study, a silicone membrane was used as a model stratum corneum and laminated dialysis membranes were placed under the silicone membrane as a model of viable skin (Wasdo *et al.*, 2009). A microdialysis probe was inserted between the dialysis membranes to determine the drug concentration in the laminated membranes (Cevc and Vierl, 2007) and flurbiprofen (FP) was used as a model drug. Since FP is applied to the skin surface as topical formulations to treat inflammation in local tissues and is highly protein-bound, the concentration profiles of FP in skin should be affected by inflammation and protein leaching in the skin (Evard *et al.*, 1996; Sugibayashi *et al.*, 1999). In the new experimental system, bovine serum albumin (BSA) solution was placed between the dialysis membranes to mimic the protein leaching in skin.

Materials and Methods

Materials

FP and BSA (Fraction V) were purchased from Sigma (St. Louis, MO). Dialysis fiber (OP-100-10) was purchased from Eicom (Kyoto, Japan). Silicone membranes (50 μm thickness) and dialysis membranes (SpectraPor 7, MWCO=1000, 50 μm thickness) were purchased from AS ONE (Osaka, Japan) and Funakoshi (Tokyo, Japan), respectively. All other

chemicals were of reagent grade.

Permeation experiments

The single membrane or laminated membranes were mounted in a 2-chamber glass diffusion cell (effective diffusion area = 0.79 cm^2, Fig. 1). The whole cell set was kept at 37^oC and FP solution (50 μg/mL for dialysis membranes or 500 μg/mL for silicone membranes, 2.8 mL) in an isotonic phosphate buffer (pH 7.0, PBS) and the buffer as a receptor medium were applied to each chamber. Samples of medium (200 – 2000 μL) in the receptor chamber were removed to determine the concentration of FP at predetermined times and fresh buffer was added to keep the volume constant. The sampling volume was chosen to keep the FP concentration in the receptor chamber low enough for sink conditions. The samples were mixed with the same volume of p-hydroxybenzoic acid iso-propyl ester (internal standard) solution in methanol (2.5 μg/mL) then the supernatant (20 μL) was subjected to HPLC (Yanagimoto *et al.*, 1998). The HPLC system consisted of a pump (LC-10AT, Shimadzu, Kyoto, Japan), an injector (7125, Rheodyne, CA), a stainless-steel column (4 x 250 mm) packed with LiChrospher 100 RP-18(e) (5 μm, Merck, Darmstadt, Germany), a UV detector (SPD-10A, Shimadzu) and an integrator (C-R5A, Shimadzu). The mobile phase consisted of 3 : 2 (v : v) acetonitrile : 0.1% phosphoric acid solution, and the flow rate was 1.0 mL/min. The detector was operated at 245 nm.

Fig. 1

The permeability coefficient (P) of FP through the membranes was calculated using the following equation.

$$P = \frac{F}{\Delta C} \qquad (1)$$

where F is the steady-state permeation rate of FP per unit area and ΔC is the concentration difference of FP between the donor and receptor phases. For the laminated membranes, the calculated P (P_{cal}) was obtained from the P of each single membrane using the following equations.

$$\frac{1}{P_{cal}} = \sum \frac{1}{P_i} \qquad (2\text{-}1)$$

$$P_{cal} = 1 \Big/ \sum \frac{1}{P_i} \qquad (2\text{-}2)$$

where P_i is P through membrane i. The obtained P_{cal} was compared with the corresponding P of the laminated membranes.

Microdialysis for the laminated membranes

The microdialysis probe was placed between the dialysis membranes as shown in Fig. 2a or b. The time schedule of microdialysis is shown in Table 1a or b and the flow rate of the dialysate was 1 μL/min. Application of FP to the laminated membrane surface was performed in the same way as in the permeation experiments. The FP concentration in each region was determined by the zero net flux method (ZNF) (Whitehead *et al.*, 2001). Briefly for Fig. 2a, using the concentration in the outflow at step 1 and step 3 in Table 1a, the concentration giving zero flux was calculated as the x-intercept of the plot of the concentration in the inflow versus the concentration difference between the inflow and outflow. At step 6 in Table 1a, the accuracy of the expected concentration was checked by verification of the zero net flux. The confidence of ZNF in the *in vitro* skin permeation experiments was given in our previous report (Seki *et al.*, 2004).

Fig. 2 and Table 1

The concentration in the region can also be calculated from Fick's law of diffusion using the following equation.

$$C_{1-2} = \frac{P_1}{P_1 + P_2} \cdot \Delta C + C_r \qquad (3)$$

where $C_{1\text{-}2}$ is the steady-state concentration in the region between the donor-side membrane (membrane 1) and the receptor-side membrane (membrane 2), C_r is the concentration in the receptor phase, and P_1 and P_2 are the permeability coefficients of membrane 1 and 2, respectively. In the

case of two dialysis membranes (Fig. 2a), the FP concentration in the region can be calculated by = $0.5 \times \Delta C + C_r$ because the concentration is the mean value of the concentration in the donor and receptor phases. In the case of skin-mimicking membranes (Fig. 2b), firstly, the FP concentration in region A in Fig. 2b was calculated using equation (3) and then the concentration in the objective region (region C in Fig. 2b, C_c) was obtained as the mean of the concentrations in regions A and C_r. If the experimental conditions were regarded as sink conditions, C_r is negligible in these calculations. These calculated concentration values were compared with the corresponding concentration values using ZNF.

Mimicking protein leaching into the membranes

In order to mimic protein leaching in skin as a pathophysiological effect of inflammation, 20 μL of BSA solution (1%) was placed in region B or D in Fig. 2b. Application of FP on the laminated membrane surface was carried out in the same way as in the permeation experiments and FP free dailysate was allowed to flow continuously at 1 μL/min. The concentration in the region C (C_c) was obtained using following equation (Kehr, 1993).

$$C_c = \frac{C_o}{1 - e^{-\left(CL_m / Q\right)}} \qquad (4)$$

where C_o is the concentration in the outflow, CL_m is the permeation clearance of the dialysis probe and Q is the flow rate of the dialysate (1 μL/min). The value of CL_m was obtained from the relationship between Q (1 - 20 μL/min) and C_o with an equilibrium FP solution (1 μg/mL) in the cell system; it was 0.330 ± 0.022 μL/min for the probe used in this study.

Results

Permeation of FP through the laminated membranes

Fig. 3a shows the permeation profiles of FP through dialysis membranes. The permeation rates

were reduced depending on the number of layers. The observed *P* values of the laminated membranes were similar to the P_{cal} values calculated from the *P* for the single membrane, suggesting that interfacial resistance between the membranes was negligible (Table 2). The permeation of FP through the single silicone membrane was about 20 times lower than that through the single dialysis membrane (Fig. 3b). The skin-mimicking membrane consisted of a single silicone membrane and four dialysis membranes showed a long lag-time although the permeation rate of FP was not very different from that through the single silicone membrane. The *P* value through the skin-mimicking membrane was similar to the P_{cal} value calculated from the observed *P* of the single silicone membrane and the laminated membranes of four dialysis membranes, and the value was about 80% of that of the single silicone membrane. Although the contribution of the viable epidermis and dermis to the permeation resistance of a full thickness skin was different for each drug and the permeability ratio of the stratum corneum to the viable epidermis and dermis depended on the physicochemical properties of the drugs, most drugs show a lower permeability for the stratum corneum than viable skin and the stratum corneum is the major rate-limiting barrier to the skin permeation of drugs (Roberts and Cross, 1999). Accordingly, the skin-mimicking membrane presented here is similar to skin, although the absolute permeability of FP was not compared with that through human skin.

Fig. 3 and Table 2

Determination of FP concentration between two dialysis membranes by ZNF

In order to verify the appropriateness of ZNF, the FP concentration between two dialysis membranes with a steady-state permeation of FP was determined (Fig. 2a). Fig. 4a shows a comparison of the permeation profiles between two simple dialysis membranes and two dialysis membranes with a dialysis probe at 1 μL/min microdialysis with PBS. The FP permeation through the membrane with dialysis was slightly lower than that without dialysis but there was no significant difference

between the permeation rates. The reduction in FP permeated is related to the permeation-resistance as the presence of the probe and removing FP into the dialysate. The amount of FP withdrawn into the dialysate was about 1 μg over 120 min and that was reasonable to explain the reduction. Anyway, the effect of dialysis on the permeation of FP was very low, and the FP concentration between two dialysis membranes can be calculated using equation (3) and can be determined by ZNF (Seki *et al.*, 2004). After the permeation experiment for 120 min, 40 μg/mL FP solution was perfused into the dialysis probe to obtain a negative net flux (steps 2 and 3 in Table 1a). The FP concentration between two dialysis membranes as the concentration giving zero flux into the dialysate was calculated as the x-intercept of the plot of the concentration in the inflow (0 and 40 μg/mL) versus the concentration difference between the inflow and outflow (9.0 $\pm$ 0.4 and -6.0 $\pm$ 0.4 μg/mL) (Fig. 4b). The obtained value was 23.9 $\pm$ 0.9 μg/mL and this was similar to that calculated by equation (3) (25 μg/mL under the assumption of sink conditions). The same FP concentration solution was prepared and the solution was perfused into the probe at steps 5 and 6 in Table 1a to evaluate the validity of this methodology. The observed FP concentration in the outflow at step 6 was 24.5 $\pm$ 0.4 μg/mL and the net flux was nearly zero, confirming the validity of ZNF.

Fig. 4

The FP concentration in region C shown in Fig. 2b for the skin-mimicking laminated membranes was also determined using ZNF. The time schedule is given in Table 1b. The cumulative amount of FP permeated through the membranes was determined for all the steps (step 0 – step 8) and is shown in Fig. 5 (-■-). The steady-state permeation rate through the membrane system dialyzed was also similar to that through the skin-mimicking membrane without dialysis (-□- in Fig. 3b), suggesting that the dialysis in the membrane system is of no consequence for such FP permeation. At steps 2 and 5, 20 μg/mL and 50 μg/mL FP solution were perfused to

obtain positive and negative values of net flux, respectively. The FP concentration in the outflow at steps 2 and 5 was 24.7 ± 0.5 μg/mL and 48.0 ± 0.6 μg/mL, respectively (Fig. 6a and Table 1b) and the net flux values were plotted to obtain the FP concentration giving zero net flux (Fig. 6b). At step 8, 41.3 ± 1.3 μg/mL of FP solution as the suggested concentration in Fig. 6b was perfused to validate the determination. The observed FP concentration in the outflow was 41.2 ± 1.8 μg/mL, also confirming the validity of this methodology. The FP concentration in region C can be calculated using equation (3) twice. Under the assumption of sink conditions, the FP concentration in region A was calculated as 67.5 μg/mL from the values of the permeability of FP through the single silicone membrane and four dialysis membranes (Table 2) first and then the FP concentration in region C was obtained as half of this value which was 33.8 μg/mL. Considering the total concentration difference of 500 μg/mL, the calculated value was reasonably close to the observed value using ZNF.

Figs. 5 and 6

Effect of BSA in the skin mimicking membrane on the permeation of FP

In inflamed tissues, vascular permeability increases and some types of proteins leach out of plasma into the extracellular space (Ortiz *et al.*, 2008). In order to imitate such situations, BSA solution was placed in region B or D in the skin-mimicking laminated membranes (Fig. 2b) and the effects on the permeation of FP were evaluated. The FP concentration in region C was determined using equation (4), not by ZNF, to obtain the concentration-time profile before steady-state. The FP permeation profiles through the membranes with BSA solution showed a long lag-time but the steady- state permeation rates were not very different from that without BSA solution (-○- and –△- in Fig. 5). No significant difference in the profiles was found for the region of BSA solution inserted. The BSA solution could work as a capacity factor to delay reaching steady- state. Fig. 7 shows the FP concentration-time profiles in region C. In the case of BSA placed in region B, the

FP concentration in region C increased gradually over 360 min and the appearance of FP in the receptor medium was proportional to the concentration in region C. Although transfer of FP from the donor to region C was interfered with BSA placed in region B, FP in region C could simply diffuse to the receptor according to Fick's law. On the other hand, the FP concentration in region C for the membrane in which BSA solution was placed in region D achieved a steady level in 120 min, although the time to achieve steady-state permeation through the laminated membranes was about 360 min. This result suggests that the amount of FP binding to BSA placed in region D increased for almost 360 min and the increase in binding suppressed the appearance of FP in the receptor phase, even if the FP concentration in region C was high enough. In both cases, the FP concentration in region C could be 35 – 40 μg/mL at steady- state and the values were close to those determined by ZNF (41.3 μg/mL) and calculated using equation (3) (33.8 μg/mL) for the membranes without BSA solution. This result suggests that BSA can work as a capacity factor to keep FP in the region but the FP concentration in the other region is unaffected by BSA. This means that the concentration-distance profiles of free (unbound) FP in the laminated membranes are not influenced by the presence of BSA at steady-state for permeation.

Fig. 7

Discussion

Although *in vitro* experimental systems using excised skins from experimental animals are generally used for studies on skin absorption of drugs, they are not suitable to evaluate the drug concentration profiles in skin because of the lack of local blood flow and physiological response. Therefore, a new skin-mimicking *in vitro* experimental system consisting of artificial membranes will be useful for basic studies on the skin absorption of drugs. In this study, a silicone membrane was used as a model stratum corneum and laminated dialysis membranes were placed under the silicone membrane

as a model of viable skin to imitate the layered structure of skin. The *P* of the laminated membranes agreed with that calculated from the *P* of the component membranes (Table 2), suggesting that the interfacial resistance between each membrane was negligible. The FP concentration in a region between the membranes was determined using ZNF to evaluate the concentration-distance profiles through the laminated membranes. The observed concentration was similar to that calculated using equation (3). These results suggest that the skin-mimicking laminated membranes represent a suitable model, giving results that agreed with Fick's law of diffusion.

In order to confirm the value of this model, as an example, the effects of BSA placed between the membranes on the permeation profiles of FP through the membranes were examined. Although protein leaching into the extracellular space of inflamed skin tissues can affect the disposition of drug in the skin, especially for highly protein-bound drugs, examination of such a complex process consisting of diffusion and binding may be difficult in *in vitro* experiments using excised skin and in *in vivo* absorption studies (Morimoto *et al.*, 2000). In this study, BSA solution was placed in two different regions (region B and D in Fig. 2b) and the effects on the permeation profiles and the concentration between the membranes (region C in Fig. 2b) were examined. Although the FP permeation profiles through the membranes with BSA solution showed a long lag-time, the steady-state permeation rates were not very different from that without BSA solution and the profiles were independent of where the BSA was located (-○- and –△- in Fig. 5). On the other hand, the FP concentration profiles in region C were different with regard to the location of BSA before steady-state, suggesting that BSA solution worked as a capacity factor to delay reaching steady-state. The concentration-distance profiles of free FP in the laminated membranes were not influenced by the presence of BSA at steady-state.

Since the dialysis membranes used as a model viable skin in the skin-mimicking laminated

membranes had a low MW cut-off (MWCO=1000), BSA placed in one region could not diffuse to the other region in the system. Although this is good for obtaining clear results, proteins leaching into the extracellular space in inflamed tissues can diffuse according to the concentration gradient in actual situations. The use of dialysis membranes having a higher MW cut-off than that of binding proteins as model viable skin will give valuable information about the contribution of proteins to drug transfer. The effects will depend on the direction of the concentration gradient of the protein itself. Using skin-mimicking laminated membranes, any direction of protein concentration gradient can be recreated in the laminated membranes. Since the viable epidermis and dermis have different cellular densities and components, the diffusion of proteins can differ depending on their extracellular aqueous space. Recently, a tight junction structure was found in the viable epidermis (Wakamatsu *et al.*, 2007; Proksch *et al.*, 2008) and this complicated our understanding of the viable epidermis with regard to drug diffusion. The tight junctions may work as specific molecular sieves for penetrants. Lamination of different types of dialysis membranes can be helpful to imitate such complicated structures of viable skin in a simple way.

In this study, the microdialysis probe was placed in the laminated membranes to determine the concentration in the local region. In another way, microdialysis probes can be used as model vessels to imitate blood flow in skin. Although the blood flow rate in skin affects the uptake of drugs from the dermis into the bloodstream, the flow rate is difficult to control in *in vivo* studies. The contributions of the interaction of drugs with components in the blood, e. g. plasma protein binding, to the drug uptake are also difficult to evaluate quantitatively. If microdialysis probes are used as model vessels, the flow rate can be controlled simply and the composition of the model blood can be chosen freely (Seki *et al.*, 2004). The microdialysis probe used was impermeable to BSA and that can generally be used to determine the concentration of unbound drugs. Another type of microdialysis probe showing permeability for BSA is commercially available. Such a

microdialysis probe can be used to determine the total concentration of drugs in a region of BSA placed in the skin-mimicking membranes. In addition, the probe can be used to imitate vessels exhibiting high permeability in inflamed tissues. If such a probe is used as a model vessel, proteins in the model blood and the medium itself will leach out into the extra vascular space in the skin-mimicking membranes. Such progressive edema can affect the permeation of drugs through the membranes.

In conclusion, skin-mimicking laminated membranes as an alternative to animal experimentation were prepared and examined as a tool for studying transdermal drug absorption. The laminated membranes are useful for obtaining quantitative results for FP permeation through membranes. In the addition, such membranes can be used to imitate some events which may occur in inflamed tissues in skin. Studies using such membranes are valuable for understanding the details of the skin absorption of drugs and to reduce the use of experimental animals.

Acknowledgment

This work was supported by Japan Society for the Promotion of Science KAKENHI (20590152).

References

Cevc, G. and Vierl, U., (2007) Spatial distribution of cutaneous microvasculature and local drug clearance after drug application on the skin, *J. Control. Release*, 118, 18-26.

Clough, G. F., Boutsiouki, P., Church, M. K., and Michel, C. C., (2002) Effects of blood flow on the in vivo recovery of a small diffusible molecule by microdialysis in human skin, *J. Pharmacol. Exp. Ther.*, 302, 681-686.

de Jager, M. W., Gooris, G. S., Ponec, M., and Bouwstra, J. A., (2005) Lipid mixtures prepared with well-defined synthetic ceramides closely mimic the unique stratum corneum lipid phase behavior, *J.*

Lipid Res., 46, 2649-2656.

Evard, P. A., Cumps, J., and Verbeeck, R. K., (1996) Concentration-dependent plasma protein binding of flurbiprofen in the rat: An in vivo microdialysis study, *Pharm. Res.*, 13, 18-22.

Kehr, J., (1993) A survey on quantitative microdialysis: theoretical models and practical implications, *J. Neurosci. Meth.*, 48, 251-261.

Morimoto, Y., Hayashi, T., Kawabata, S., Seki, T., and Sugibayashi, K., (2000) Effect of l-menthol-ethanol-water system on the systemic absorption of flurbiprofen after repeated topical applications in rabbits, *Bio. Pharm. Bull.*, 23, 1254-1257.

Ortiz, P. G., Hansen, S. H., Shah, V. P., Menne, T., and Benfeldt, E., (2008) The effect of irritant dermatitis on cutaneous bioavailability of a metronidazole formulation, investigated by microdialysis and dermatopharmacokinetic method, *Contact Dermatitis*, 59, 23-30.

Ortiz, P. G., Hansen, S. H., Shah, V. P., Menne, T., and Benfeldt, E., (2009) Impact of adult atopic dermatitis on topical drug penetration: Assessment by cutaneous microdialysis and tape stripping, *Acta Derm. Venereol.*, 89, 33-38.

Ottaviani, G., Martel, S., and Carrupt, P.-A., (2006) Parallel artificial membrane permeability assay: A new membrane for the fast prediction of passive human skin permeability, *J. Med. Chem.*, 49, 3948-3954.

Proksch, E., Brandner, J. M., and Jensen, J. M., (2008) The skin: an indispensable barrier, *Exp. Dermatol.*, 17, 1063-1072.

Roberts, M. S. and Cross, S., (1999) Percutaneous absorption of topically applied NSAIDS and other compounds: Role of solute properties, skin physiology and delivery systems, *Inflammopharmacol.*, 7, 339-350.

Russell, L. M. and Guy, R. H., (2009) Measurement and prediction of the rate and extent of drug delivery into and through the skin, *Expert Opin. Drug Deliv.*, 6, 355-369.

Touitou, E., Meidan, V. M., and Horwitz, E., (1998) Methods for quantitative determination of drug localized in the skin, *J. Control. Release*, 56, 7-21.

Seki, T., Hosoya, O., Yamazaki, T., Sato, T., Saso, Y., Juni, K., and Morimoto, K., (2004) A rabbit ear flap perfusion experiment to evaluate the percutaneous absorption of drugs, *Int. J. Pharm.*, 276, 29-40.

Seki, T., Wang, A., Yuan, D., Saso, Y., Hosoya, O., Chono, S., and Morimoto, K., (2004) Excised porcine skin experimental systems to validate quantitative microdialysis methods for determination of drugs in skin after topical application, *J. Control. Release*, 100, 181-189.

Shukla, C., Patel, V., Juluru, R., and Stagni, G., (2009) Quantification and prediction of skin pharmacokinetics of amoxicillin and cefuroxime, *Biopharm. Drug Dispos.*, in press.

Sugibayashi, K., Yanagimoto, G., Hayashi, T., Seki, T., Juni, K., and Morimoto, Y., (1999) Analysis of skin disposition of flurbiprofen after topical application in hairless rats, *J. Control. Release*, 62, 193-200.

Wakamatsu, K., Ogita, H., Okabe, N., Irie, K., Okamoto, M. T., Ishizaki, H., Yamamoto, A. I., Iizuka, H., Miyoshhi, J., and Takai, Y., (2007) Up-regulation of loricrin expression by cell adhesion molecule Nectin-1 through Rap 1-ERK signaling in keratinocytes, *J. Biol. Chem.*, 282, 18173-18181.

Wasdo, S. C., Juntunen, J., Devarajan, H., and Sloan, K. B., (2009) A correlation of flux through a silicone membrane with flux through hairless mouse skin and human skin in vitro, *Int. J. Pharm.*, 373, 62-67.

Whitehead, K. J., Manning, J.-P., Smith, C. G. S., and Bowery, N. G., (2001) Determination of the extracellular concentration of glycine in the rat spinal cord dorsal horn by quantitative microdialysis, *Brain Res.*, 910, 192-194.

Yanagimoto, G., Hayashi, T., Seki, T., Juni, K., Sugibayashi, K., and Morimoto, Y., (1998) A new

in-situ experimental method to evaluate the cutaneous disposition of flurbiprofen after topical application in hairless rats, *Pharm. Pharmacol. Commun.*, 4, 1-5.

Table 1 Time schedules for microdialysis

(a) Schedule for Fig. 2a set up

	Time (min)	Flow (μL/min)	inflow (μg/mL)	outflow (μg/mL)	out-in (μg/mL)
step 0	0-20	1	0	-	-
step 1	20-120	1	0	8.96±0.39	8.96±0.39
step 2	120-140	1	40	-	-
step 3	140-170	1	40	34.0±0.4	-6.0±0.4
step 4	170-200	-	-	-	-
step 5	200-220	1	23.9±0.9	-	-
step 6	220-250	1	23.9±0.9	24.5±0.4	0.5±0.6

Data are expressed as mean ±SD (n=3).

(b) Schedule for Fig. 2b set up

	Time (min)	Flow (μL/min)	inflow (μg/mL)	outflow (μg/mL)	out-in (μg/mL)
step 0	0-30	-	-	-	-
step 1	30-60	1	20	-	-
step 2	60-90	1	20	24.7±0.5	4.7±0.5
step 3	90-120	-	-	-	-
step 4	120-150	1	50	-	-
step 5	150-180	1	50	48.0±0.6	-2.0±0.6
step 6	180-210	-	-	-	-
step 7	210-240	1	41.3±1.3	-	-
step 8	240-270	1	41.3±1.3	41.2±1.8	-0.1±0.6

Data are expressed as mean ±SD (n=3).

Table 2 Observed and calculated permeability coefficients of FP through single or laminated membranes

	Observed permeability (cm/min)	Calculated permeability (cm/min)
Single dialysis membrane	$3.76\times10^{-3}\pm0.11\times10^{-3}$	-
Two dialysis membranes	$1.90\times10^{-3}\pm0.17\times10^{-3}$	1.88×10^{-3} [a]
Three dialysis membranes	$1.39\times10^{-3}\pm0.03\times10^{-3}$	1.25×10^{-3} [a]
Four dialysis membranes	$1.14\times10^{-3}\pm0.10\times10^{-3}$	0.94×10^{-3} [a]
Five dialysis membranes	$0.87\times10^{-3}\pm0.05\times10^{-3}$	0.75×10^{-3} [a]
Single silicone membrane	$1.78\times10^{-4}\pm0.08\times10^{-4}$	-
Silicone membrane with four dialysis membranes	$1.45\times10^{-4}\pm0.16\times10^{-4}$	1.54×10^{-4} [b]

a: Calculated using the observed value of the single dialysis membrane.

b: Calculated using the observed value of the single silicone membrane and four dialysis membranes.

Data are expressed as mean ±SD (n=3).

Fig. 1

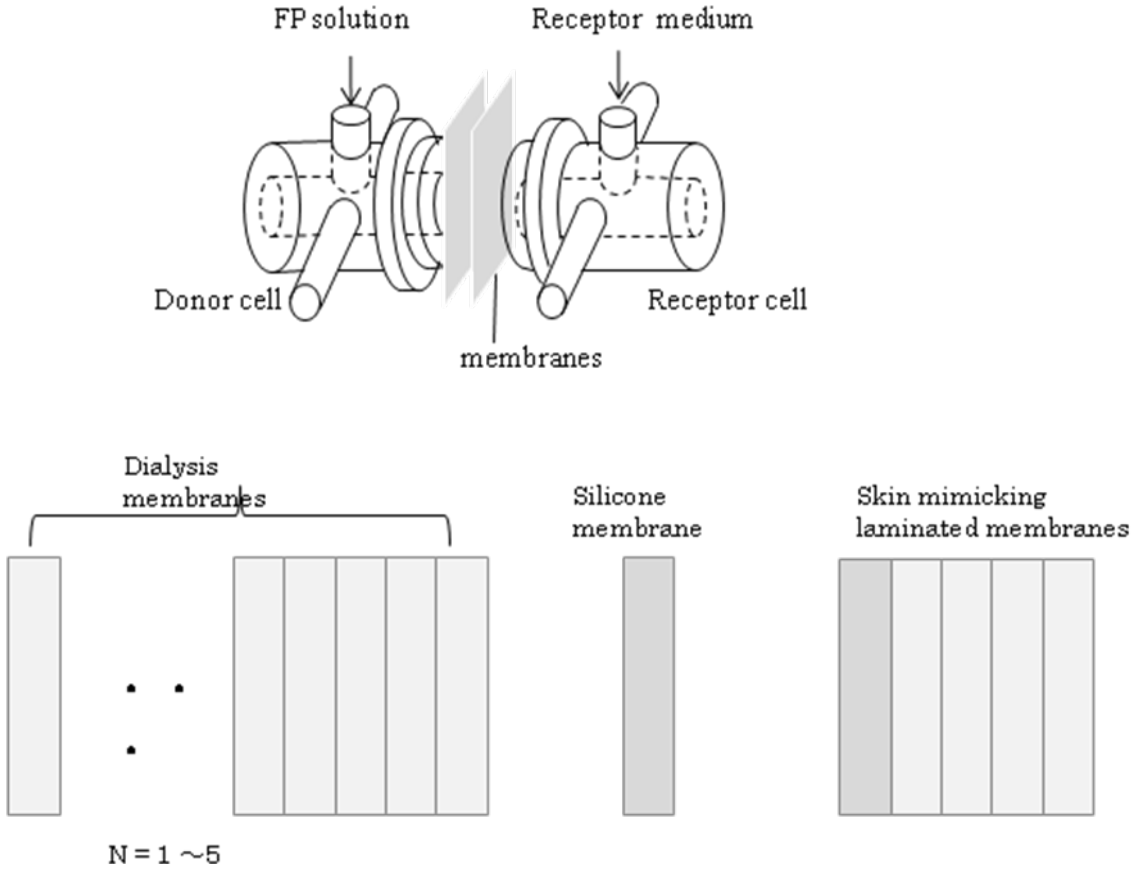
FP solution
Receptor medium
Donor cell
Receptor cell
membranes
Dialysis membranes
Silicone membrane
Skin mimicking laminated membranes
N = 1 ～5

Fig. 2

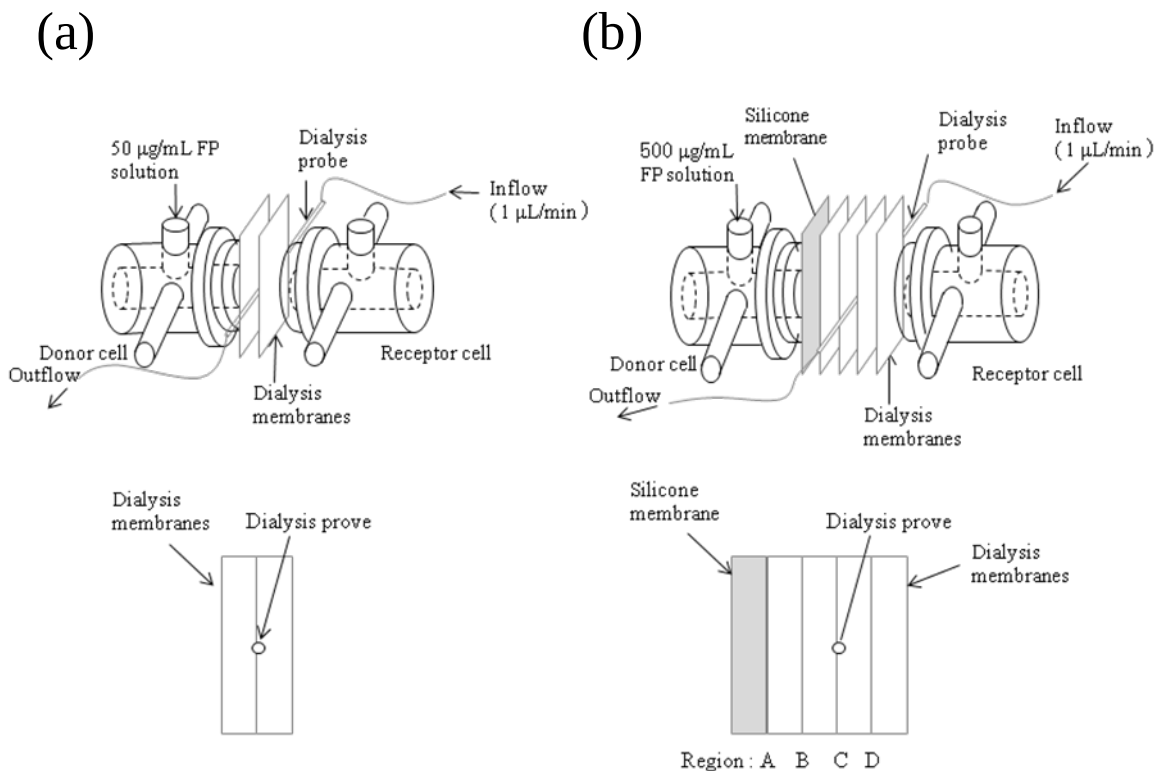
(a)
50 μg/mL FP solution
Dialysis probe
Inflow (1 μL/min)
Donor cell
Outflow
Receptor cell
Dialysis membranes
Dialysis membranes
Dialysis prove
(b)
Silicone membrane
500 μg/mL FP solution
Dialysis probe
Inflow (1 μL/min)
Donor cell
Outflow
Receptor cell
Dialysis membranes
Silicone membrane
Dialysis prove
Dialysis membranes
Region : A B C D

Fig. 3

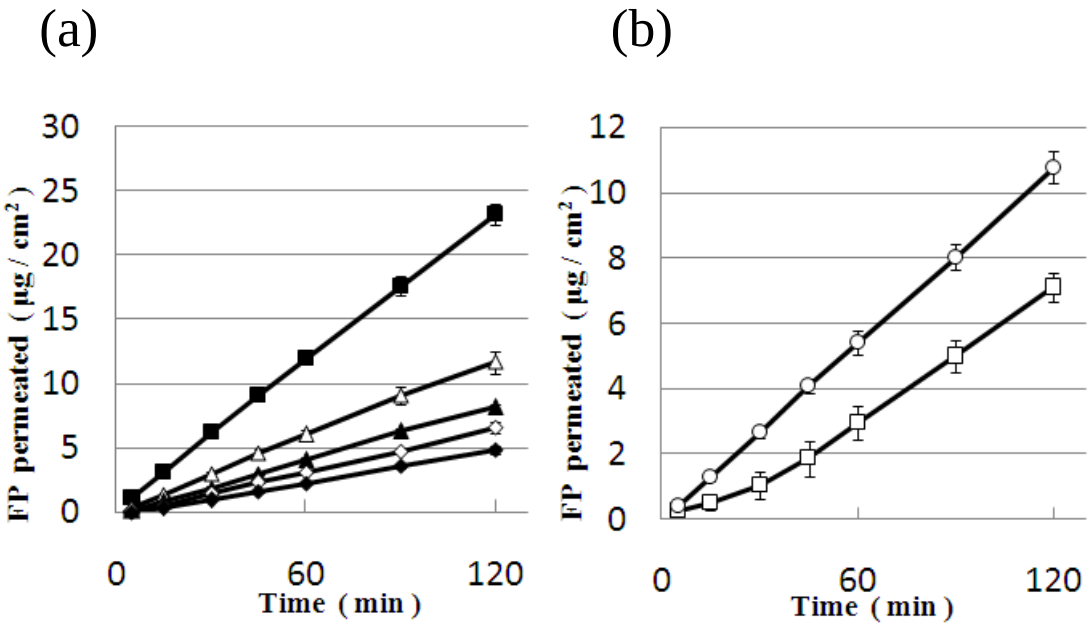
(a)
(b)
FP permeated (μg / cm2)
30
25
20
15
10
5
0
0
60
120
Time (min)
FP permeated (μg / cm2)
12
10
8
6
4
2
0
0
60
120
Time (min)

Fig. 4

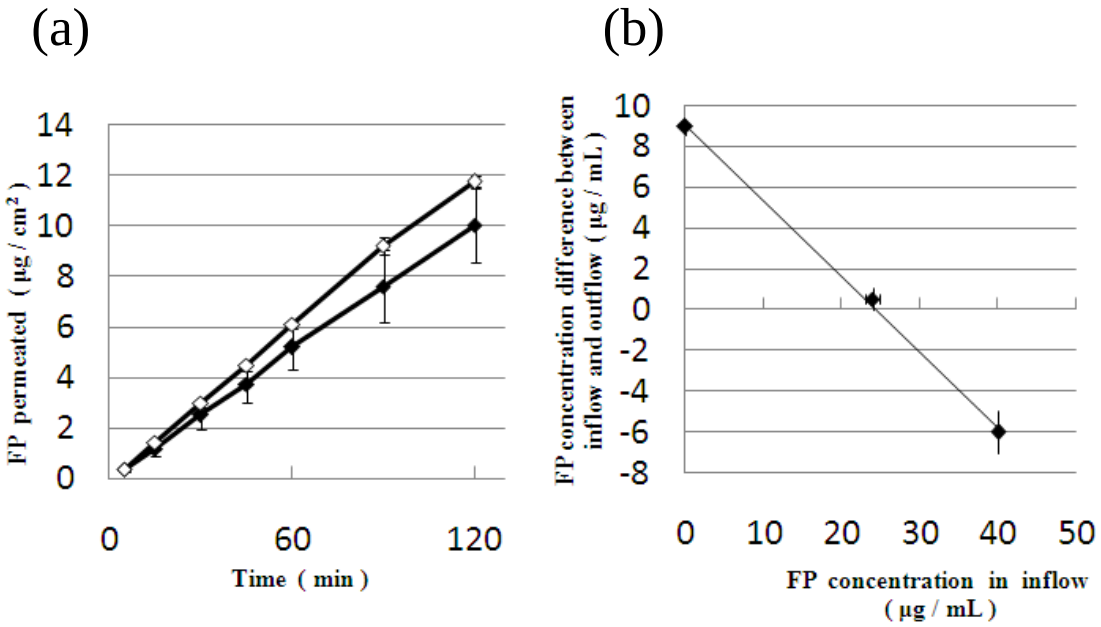
(a)
(b)
FP permeated (μg / cm²)
14
12
10
8
6
4
2
0
0
60
120
Time (min)
FP concentration difference between inflow and outflow (μg / mL)
10
8
6
4
2
0
-2
-4
-6
-8
0
10
20
30
40
50
FP concentration in inflow (μg / mL)

Fig. 5

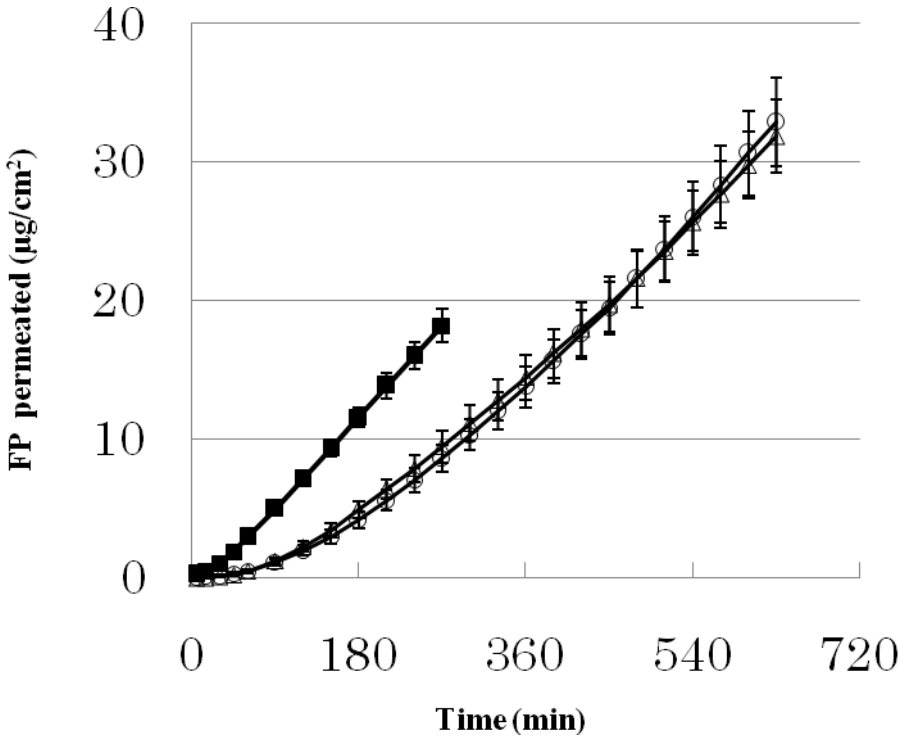

Fig. 6

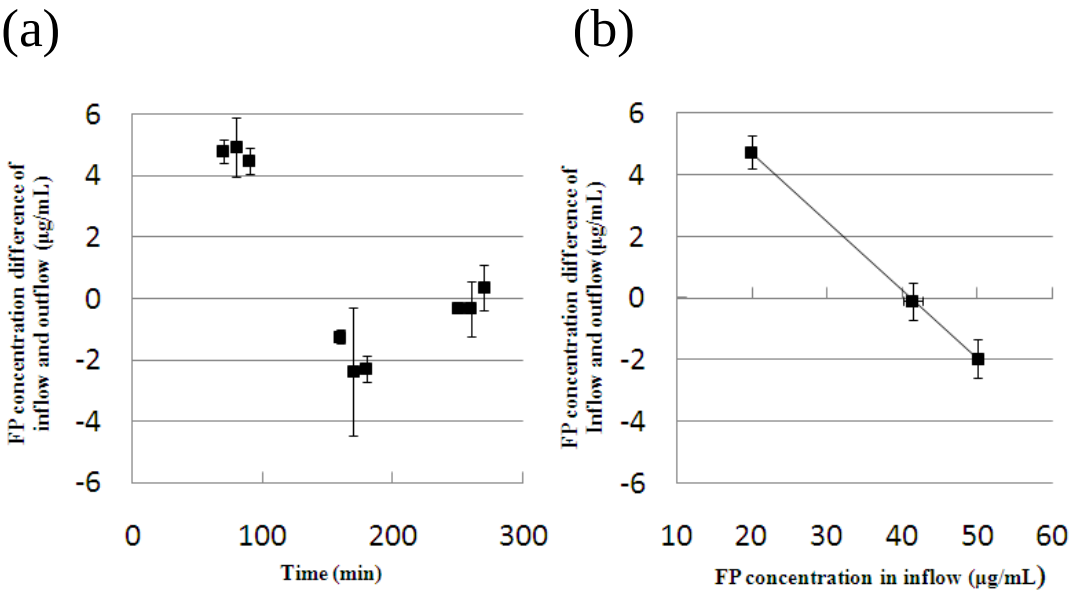
(a)
(b)
FP concentration difference of inflow and outflow (μg/mL)
6
4
2
0
-2
-4
-6
0
100
200
300
Time (min)
FP concentration difference of Inflow and outflow (μg/mL)
10
20
30
40
50
60
FP concentration in inflow (μg/mL)

Fig. 7

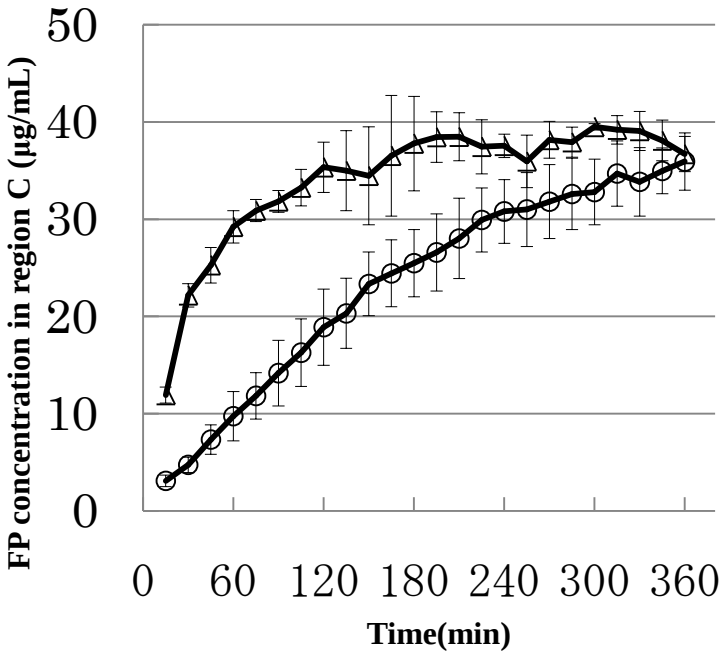
50
40
30
20
10
0
FP concentration in region C (μg/mL)
0
60
120
180
240
300
360
Time(min)

Figure Legends

Fig. 1 Permeation experiments set up for single or laminated membranes

Fig. 2 Permeation experiments set up with microdialysis

(a) Two dialysis membranes

(b) Single silicone membrane and four dialysis membranes (skin-mimicking membrane)

Fig. 3 Permeation profiles of FP through single or laminated membranes

(a) ■, single dialysis membrane; △, two dialysis membranes; ▲, three dialysis membranes; ◇, four dialysis membranes; ◆, five dialysis membranes.

(b) ○, single silicone membrane; □, single silicone membrane and four dialysis membranes = skin-mimicking membrane.

Data are expressed as mean ±SD (n=3).

Fig. 4 Application of microdialysis for permeation of FP through two dialysis membranes

(a) Effect of microdialysis on the permeation profiles of FP: ◇, FP permeation without microdialysis; ◆, FP permeation with microdialysis (FP free solution, 1 μL/min).

(b) Net flux plots of FP to determine the FP concentration giving zero net flux: the x-intercept giving zero net flux means the expected FP concentration in the region the probe is located (region C in Fig. 2b).

Data are expressed as mean ±SD (n=3).

Fig. 5 Effects of BSA solution placed between dialysis membranes in the skin-mimicking membrane on the permeation profiles of FP with microdialysis

■, without BSA solution; ○, BSA solution (1%, 20 μL) in region B in Fig. 2b; △, BSA solution (1%, 20 μL) in region D in Fig. 2b.

Data are expressed as mean ±SD (n=3).

Fig. 6 Microdialysis evaluation for FP permeation through the skin-mimicking membrane

(a) FP concentration in the outflow (Table 1b).

(b) Net flux plots of FP to obtain the FP concentration giving zero net flux: the x-intercept giving zero net flux means the expected FP concentration in the region the probe was placed (region C in Fig. 2b).

Data are expressed as mean ±SD (n=3).

Fig. 7 FP concentration-time profiles in region C in Fig 2b for FP permeation through the skin-mimicking membrane with BSA solution

○, BSA solution (1%, 20 μL) in region B in Fig. 2b; △, BSA solution (1%, 20 μL) in region D in Fig. 2b. The FP concentration was calculated using equation (4).

Data are expressed as mean ±SD (n=3).